



## Modal Parameter Estimation of Tall Structures using HHT with Improved EMD

K Lakshmi<sup>1\*</sup>, Varun Kasi Reddy<sup>2</sup> and A Rama Mohan Rao<sup>1</sup>

<sup>1</sup>CSIR-Structural Engineering Research Centre, CSIR Campus, Taramani, Chennai 600 113, Tamilnadu, India

<sup>2</sup>Dept of Civil and Environmental Engineering, Carnegie Mellon University, Pittsburgh, PA 15213, United States

*Received 06 September 2020; revised 03 February 2022; accepted 06 May 2022*

In this paper, identification of the natural frequencies, damping ratios and mode shapes of the structures using the measured ambient responses are proposed using time-frequency analysis. The impulse responses are obtained from the measured acceleration time history data through cross-correlations. Empirical Mode Decomposition (EMD) is employed on these generated impulse responses to obtain Intrinsic Mode Functions (IMFs). Finally, modal identification of the structure is carried out by performing Hilbert Transform (HT) on these generated IMFs. To avoid the problem of mode mixing during EMD of the signal, an improved version with intermittency criteria along with treatment to end effects during sifting is proposed in this paper. Experimentally measured data of Guangzhou New TV (GNTV) Tower is used to test and verify the proposed algorithm. The studies indicate that the proposed HHT based algorithm can be applied quite effectively for the modal identification of practical engineering structures.

**Keywords:** GNTV tower, Modal identification, Non-stationary ambient response, Time-frequency analysis

### Introduction

Accurate estimation of modal parameters are essential for important tall buildings/towers subjected to strong wind or earthquake loads and also bridges under ambient loads to predict the true response of these structures. Apart from this vibration-based structural health monitoring techniques also require the accurate assessment of these modal parameters to characterize the damages in the structures. The structural damping is rather difficult to estimate for long-span bridges and tall built-up structures. However, damping plays a major role in the measured structural response due to external excitations.

Ambient vibration tests are often carried out on civil engineering structures like buildings and bridges to obtain the required dynamic responses. Since it is difficult to measure the ambient input forces which include natural forces like wind, and earthquake excitations, several algorithms are developed for structural modal identification using the measured ambient response data.

Time domain based techniques for modal identification are more popular and are being widely used. Since the proposed algorithm also comes under the time domain, we focus more on the time domain

algorithms. Since these time domain algorithms work more effectively with impulse responses derived from the measured ambient responses, random decrement technique<sup>1</sup> is popularly being used to preprocess and convert the ambient raw measured data to free decay responses. Modal parameters are subsequently estimated using these free decay responses by employing the traditional time domain methods.<sup>2,3</sup> However, later time series models based techniques<sup>4,5</sup> are proposed, which can directly use the measured ambient vibration responses for modal parameter identification. Stochastic Subspace Identification (SSI)<sup>6</sup>, Natural EXcitation Technique with the Eigen system Realization Algorithm (NEXT-ERA)<sup>7</sup>, Blind Source Separation (BSS)<sup>8</sup> and an online modal extraction technique based on Bayesian formulation<sup>9</sup> are some of the recently reported techniques in the literature. All these recently proposed algorithms are being widely used for modal parameter extraction of practical engineering structures. Modal identification using Autoregressive (AR), SSI, NEXT-ERA and BSS methods is carried out with the assumption that the measured responses are obtained from structures subjected to white noise excitations. Even though BSS and Autoregressive with Moving Average (ARMA) based techniques can work without such strict assumptions, they are much more complex when compared to the other algorithms listed. The major

\*Author for Correspondence  
E-mail: lakshmik@serc.res.in

issues with the majority of the aforementioned algorithms lie in the discrimination of structural modes and also the determination of modal order. Among the modes extracted, spurious (or computational) modes also will be present apart from physical modes of the structure and it becomes difficult to distinguish them. These computational or rather spurious modes account for the noise present in the signal, leakage, non-linearity and other characteristics which are not modelled. Several modal validation techniques and also an array of modal indicators are reported in the literature to distinguish the structural modes from the other spurious modes. Stability diagrams are being popularly used for this purpose. However, over the years of investigations on the aforementioned techniques indicate that these are moderately successful and several limitations still exist while extracting modal parameters for practical engineering structures. Some of such limitations are outlined here. If any dominant frequency apart from white Gaussian noise is present in the excitation force, then it is difficult to isolate such frequencies from the structural natural frequencies while using methods like SSI. As mentioned earlier, SSI works under the assumption that excitation force is Gaussian white noise. Most of these Operational Modal Analysis (OMA) techniques exhibit considerable difficulty in extracting closely spaced modes of the structure. The majority of the discussed OMA techniques are finally reduced to a set of simultaneous equations and least square techniques are generally employed to solve. Therefore due to measurement noise and leakage errors during measurements, there is a strong possibility of bias and variance errors creeping into the solutions. Further, the majority of the aforementioned techniques suffer from severe inaccuracies in modal identification, when applied to complex structures with active or passive dampers. Similar problems exist with high or moderately high damped structures<sup>10</sup> and also with closely spaced modes. Because of the above limitations, researchers are currently looking at techniques based on time scale analysis like wavelet-based techniques and time-frequency analysis like Hilbert Huang Transform based techniques with more interest.<sup>11-13</sup>

Among several choices of time-frequency analysis like Short Term Fourier Transform (STFT), Hilbert Huang Transform (HHT), wavelets etc., HHT<sup>14</sup> is widely being applied to process the vibration responses of civil engineering structures which in

most instances happens to be non-stationary signals.<sup>12</sup> HHT has drawn much attention in recent times for structural parameter identification as it has better frequency resolution to evaluate natural frequencies with very low energy leakage.<sup>15</sup> It is also reported that in comparison with other time-frequency analysis, HHT is more immune to the noise present in the measured signals.<sup>16</sup>

HHT is employed to identify modal parameters of multi-degrees of freedom structures using free vibration responses and is later extended to determine system parameters like modal stiffness, modal mass and modal damping matrices of the structures.<sup>17,18</sup> Modal identification techniques using ambient vibration responses are later developed by employing HHT on free responses obtained by pre-processing the measured time history signals with random decrement technique.<sup>19</sup> Subsequently, modal parameters of tall buildings are identified based on HHT using measured ambient wind vibration data.<sup>19</sup> The Sutong Cable-Stayed Bridge is monitored for one year using HHT by Mao *et al.*<sup>20</sup> to investigate the long term variations in the modal frequencies. Similarly, HHT is combined with variation mode decomposition for modal parameter estimation of structures by Bagheri *et al.*<sup>21</sup> Apart from this, HHT is successfully employed for Structural Health Monitoring (SHM) including railway bridges, bearing faults in induction machines, safety of beam ridge structures under vehicular load etc.<sup>22-25</sup>

Despite reporting several successful applications of HHT for engineering structures, still, several issues remain to be addressed while using HHT. One of the major issues is that EMD suffers from mode mixing and end effects because of the influence of cubic spline interpolation, which significantly affects the identification accuracy of HHT. In the proposed HHT based modal identification technique we use an improved EMD procedure with intermittency criteria to handle mode mixing. Similarly, end effects are handled using the signal extension technique based on a second-order autoregressive model. Apart from that, we use cross-correlated responses to obtain free responses from ambient vibration data instead of the RD technique traditionally being employed in HHT based modal identification methods. Detailed analytical formulations are also presented in this paper to show the effectiveness of the cross-correlated responses in effectively handling noise, stationary and non-stationary components of the measured signals.

Therefore, the proposed HHT based modal identification method is less sensitive to measurement noise. The measured ambient acceleration time history responses of the GNTV tower are used to evaluate the performance of the proposed algorithm.

**Theoretical Considerations**

**Hilbert–Huang Transform (HHT)**

The HHT on a signal is performed in two steps. In the first step, the signal is first split into several mono component signals using an empirical method, it is called Empirical Mode Decomposition (EMD). The time-frequency resolution of the signal is obtained by performing Hilbert-Transform (HT) on each of the monocomponent signals generated in the first step. Empirical Mode Decomposition<sup>14</sup> is a self-adaptive multi-resolution signal decomposition technique. It splits adaptively a complex signal without any prior knowledge of its frequency contents, into a set of oscillatory mono components called Intrinsic Mode Functions (IMFs), from the high frequency to low frequency by a process known as sifting. These IMFs will have the same numbers (or almost differing by one) of zero-crossings and extreme, and also have symmetric envelopes defined by local maxima and minima respectively. In the EMD process, the local maxima and minima points of the signal  $z(t)$  are first identified and then, using cubic spline interpolation, envelopes for these identified local maxima and minima are formed. The moving mean values of these two envelopes are evaluated and subtracted from the signal,  $z(t)$ . This process called sifting is repeated until the subtracted signal  $zc_1(t)$  is qualified as IMF by satisfying the two conditions mentioned earlier. Once  $zc_1(t)$  is obtained, the residual signal is evaluated by subtracting  $zc_1(t)$  from the original signal  $z(t)$ . Similarly, by repeating the above sifting process on the residual, the next IMF,  $zc_2(t)$  is obtained. The rest of all the desired IMFs are determined by repeatedly using this sifting process. Combining all the IMFs and the residual  $rs_m(t)$ , the original signal can be generated

$$z(t) = \sum_{k=1}^m zc_k(t) + rs_m(t) \quad \dots (1)$$

Once the IMFs are obtained from the measured time history response  $z(t)$ , Hilbert Transform (HT) can be employed on each of the generated IMFs. The HT of a real-valued function  $C_j(t)$  in the range  $-\infty < t < \infty$  defined as

$$\tilde{z}_k(t) = HT|zc_k(t)| = \frac{1}{\pi} \int_{-\infty}^{\infty} \frac{zc_k(\tau)}{t - \tau} d\tau \quad \dots (2)$$

The complex time signal  $\tilde{z}_k(t)$  can be constructed as

$$\tilde{z}_k(t) = zc_k(t) + j \tilde{z}_k(t) = a_k(t)e^{j\theta(t)} \quad \dots (3)$$

$$a_k(t) = \sqrt{([zc_k(t)]^2 + [\tilde{z}_k(t)]^2)} \quad \dots (4)$$

$$\theta_k(t) = \arctan \left[ \frac{HT(zc_k(t))}{zc_k(t)} \right] \quad \dots (5)$$

$$\omega_k(t) = \frac{d\theta_k(t)}{dt} = \frac{zc_k(t) \cdot \frac{d(HT(zc_k(t)))}{dt} - \frac{d(zc_k(t))}{dt} HT(zc_k(t))}{(a_k(t))^2} \quad \dots (6)$$

where,  $a_k(t)$ ,  $\theta_k(t)$ , and  $\omega_k(t)$  are the instantaneous amplitude, phase and frequency, of the  $k^{\text{th}}$  IMF respectively. We can represent the originally measured time history signal of  $n^{\text{th}}$  sensor node (without the residue,  $r_n(t)$ ) as the real part of the sum of the Hilbert transforms of all the IMFs generated using EMD.

$$z(t) = \text{Re} \sum_{k=1}^m a_k(t) \exp \left[ j \int \omega_k(t) dt \right] \quad \dots (7)$$

Eq. (7) gives the time-frequency resolution of the time history signal  $z(t)$  and is called as Hilbert spectrum,  $H(\omega, t)$ . The time-frequency resolution of a nonlinear and/or non-stationary signal can be identified using this Hilbert spectrum.

**Cross-Correlation of Time History Signals**

The measured vibration responses of structures will inevitably be corrupted with measurement noise. Because of this, the system or modal identification techniques need to be more immune to the measurement noise. Otherwise, the identification results may be highly distorted due to noise. The measured noise corrupted responses obtained from a sensor placed on the structure can be written as

$$\tilde{z}(t) = z(t) + \xi(t) \quad \dots (8)$$

where,  $\tilde{z}(t) = [\tilde{z}_1(t), \tilde{z}_2(t), \dots, \tilde{z}_n(t)]^T$  is the measured acceleration time history response of the structure. As mentioned earlier, these responses are corrupted with measurement noise.  $z(t) = [z_1(t), z_2(t), \dots, z_n(t)]^T$  is the noise-free acceleration time history response and  $\xi(t) = [\xi_1(t),$

$\xi_2(t), \dots, \xi_n(t)$  is the zero mean unit variance ( $\sigma^2$ ) Gaussian white noise.

Let us choose two typical spatial locations, say ‘r’ and ‘s’ where the accelerometers are placed on the structure. The cross-correlated responses,  $R_{rs}$ , of the time history measurements at locations ‘r’ and ‘s’ can be evaluated as

$$\begin{aligned} R_{rs}(\tilde{z}_r(t), \tilde{z}_s(t + \tau)) &= E[\tilde{z}_r(t), \tilde{z}_s(t + \tau)] \\ &= E[(z_r(t) + \xi_r(t)), (z_s(t + \tau) + \xi_s(t + \tau))] \\ &= E[z_r(t) z_s(t + \tau)] + E[z_r(t) \xi_s(t + \tau)] + \\ &E[z_s(t + \tau) \xi_r(t)] + E[\xi_r(t) \xi_s(t + \tau)] \quad \dots (9) \end{aligned}$$

In the above equation, the terms  $E[z_r(t) \xi_s(t + \tau)]$  and  $E[z_s(t + \tau) \xi_r(t)]$  will vanish as the time history responses and the measurement noise are uncorrelated. Similarly, the term  $E[\xi_r(t) \xi_s(t + \tau)]$  will also vanish when  $\tau \neq 0$  and  $E[\xi_r(t) \xi_s(t + \tau)] = \sigma^2$ , when  $\tau = 0$ .  $\sigma^2$ , is the variance of the measurement noise.

The ambient excitation,  $f(t)$  consists of stationary,  $f_{st}(t)$ , non-stationary,  $f_{nst}(t)$ , random components. Similarly, the nonstationary component is a combination of periodic,  $f_{nst}^p(t)$ , and periodic,  $f_{nst}^{\bar{p}}(t)$ , components. Accordingly, the external ambient excitation,  $f(t)$ , can be represented in the split form as.

$$f(t) = f_{st}(t) + f_{nst}^p(t) + f_{nst}^{\bar{p}}(t) \quad \dots (10)$$

Generally, if  $E[f_{st}^2(t)] \gg E[f_{nst}^2(t)]$ , the excitation is considered stationary, else, it is nonstationary. Similarly, the measured structural responses will also contain both stationary and nonstationary components corresponding to stationary and nonstationary components of ambient excitations. Therefore, the responses can also be split similar to the ambient excitation given in Eq. (10). Accordingly, the structural responses at sensor locations ‘r’ and ‘s’ in the split form are

$$\begin{aligned} z_r(t) &= z_r^{st}(t) + Z_r^p(t) + Z_r^{\bar{p}}(t); \\ z_s(t) &= z_s^{st}(t) + Z_s^p(t) + Z_s^{\bar{p}}(t) \quad \dots (11) \end{aligned}$$

The response components subjected to random stationary, periodic and aperiodic excitations are represented with superscripts ‘st’, ‘p’, and  $\bar{p}$  respectively in Eq. (11). The cross-correlated

response corresponding to sensor nodes ‘r’ and ‘s’ given in Eq. (11) can be written as

$$\begin{aligned} R_{rs}(t_1, t_2) &= E[z_r(t_1) z_s(t_2)] \\ &= E[z_r^{st}(t_1) z_s^{st}(t_2)] + E[z_r^p(t_1) z_s^p(t_2)] + \bar{r}_{rs}(t_1, t_2) \quad \dots (12) \end{aligned}$$

$$\begin{aligned} \text{where, } \bar{r}_{rs}(t_1, t_2) &= E[z_r(t_1) z_s(t_2)] - E[z_r^{st}(t_1) z_s^{st}(t_2)] \\ &\quad - E[z_r^p(t_1) z_s^p(t_2)] \quad \dots (13) \end{aligned}$$

We can write the stationary and periodic components from Eq. (13) as

$$\begin{aligned} R_{rs}^{st}(\tau) &= E[z_r^{st}(t) z_s^{st}(t + \tau)] = \sum_{j=1}^{n_s} B_{rs}^j e^{-\zeta^j(t)\omega^j(t)\tau} \dots \\ &\times \sin(\omega_d^j(t)\tau + \phi_j) \quad \dots (14) \end{aligned}$$

$$\begin{aligned} R_{rs}^p(\tau) &= E[z_r^p(t_1) z_s^p(t_2)] = \sum_{h=n_s+1}^{n_s+k} B_{rs}^h e^{-\zeta^h\omega^h\tau} \dots \\ &\times \sin(\omega_d^h\tau + \phi_h) \quad \dots (15) \end{aligned}$$

where,  $n_s$  and  $k$  represent the total number of exciting frequencies by the stationary and periodic excitations respectively.  $B_{rs}$  represent the modal coefficient of nodes r and s.  $\omega$  is the natural frequency. Similarly,  $\omega_d, \zeta$ , and  $\phi$  are the damped natural frequency, damping ratio, and the phase respectively, of the corresponding mode. The superscripts  $j$  and  $h$  represent the frequency number excited by the stationary and periodic random excitations respectively. Combining the Eqs (14) and (15) which are similar, and adding the remaining noise component, Eq. (12), can be conveniently represented as

$$R_{rs}(\tau) = \sum_{j=1}^{n_s+k} C_{rs}^j e^{-\zeta^j \omega^j(t)\tau} \sin(\omega_d^j(t)\tau + \phi_j) + \bar{r}_{rs}(t_1, t_2) \quad \dots (16)$$

where,  $C_{rs}^j$  is the amplitude of the  $j^{\text{th}}$  mode of the response  $R_{rs}$ . Using EMD on Eq. (16) finite number of IMFs and a residue can be generated

$$R_{rs}(\tau) = \sum_{j=1}^{n_s+k} M_{rs}^j(\tau) + r(\tau) ; \quad \dots (17)$$

where,  $\sum_{j=1}^{n_s+k} M_{rs}^j(\tau) = \sum_{j=1}^{n_s+k} C_{rs}^j e^{-\zeta^j \omega^j(t)\tau} \sin(\omega_d^j(t)\tau + \phi_j)$  and residue  $r(\tau) = \bar{r}_{rs}(t_1, t_2)$ . This residual part consists of measurement noise and also the components of the

response which do not contain the modal information i.e., response under aperiodic excitations. From this formulation, it is clear that using the cross-correlated responses, the time history response of a structure under ambient excitation (consists of both stationary and nonstationary components) can be split into a finite set of IMFs using empirical mode decomposition. We also notice that non-modal components of the response including noise can be conveniently isolated to a larger extent using this formulation. Taking time difference T as a variable, the first IMF,  $C_{rs}^j(t)$  can be written as:

$$C_{rs}^j(\tau) = \left| B_{rs}^j \right| e^{-\zeta_j \omega_n^j(t)T} \sin(\omega_d^j(\tau) + \phi_r^j) \quad \dots (18)$$

Hilbert transform of the first IMF,  $C_{rs}(T)$ , denoted by  $\tilde{C}_{rs}(T)$  can be obtained as

$$Z_{rs}^j(T) = C_{rs}^j(T) + i\tilde{C}_{rs}^j(T) = A_{rs}^j(T)e^{i\theta_{rs}^j(T)} \quad \dots (19)$$

where,  $A_{rs}^j(T) = \left| B_{rs}^j \right| e^{-\zeta_j \omega_n^j(t)T} \quad \dots (20)$

$$\theta_{rs}^j(T) = \omega_d^j(t)T + \phi_r^j \quad \dots (21)$$

From Eqs (20) and (21), we can obtain

$$\frac{d \ln A_{rs}^j(T)}{dT} = -\zeta_j \omega_n^j(t) \quad \dots (22)$$

$$\omega^j = \frac{d\theta_{rs}^j(T)}{dT} = \omega_d^j \quad \dots (23)$$

The slope of the ‘phase angle  $\theta_{rs}^j$  Vs time’ plot is evaluated using the linear least-squares technique<sup>12</sup> to compute  $\omega_d^j$ . Similarly, using the plot ‘ $\ln A_{rs}^j(T)$  Vs time’, the decaying amplitude slope  $-\zeta_j \omega_n^j$  is evaluated. The desired modal parameters can be evaluated using these two values as

$$\zeta_1 = -\zeta_j \omega_n^j \quad \text{and} \quad \zeta_2 = \omega_d^j = \omega_n^j \sqrt{1 - \zeta_j^2} \quad \dots (24)$$

$$\zeta_j = \sqrt{\frac{\zeta_1^2}{\zeta_1^2 + \zeta_2^2}} \quad \dots (25)$$

$\omega_n^j$  can be obtained from Eq. (24).

**EMD with Intermittency**

The non-stationary time history signal reconstructed using HHT are complete, orthogonal, local and adaptive. Therefore the IMFs generated

through EMD should also reflect these properties. However, the IMFs generated using sifting cannot ensure good quality. It is mainly due to the large swings at both ends of the signal, due to the spline fitting process during sifting. These spurious swings propagate to the inner portions of the signal and distract it completely. This ultimately results in producing poor intrinsic mode functions.

The large swings are more prominent particularly when the components of lower frequencies are contained in the signal. Apart from this, the quality of sifting will be inferior, especially in the signals with closely spaced frequencies. In this case, the generated IMFs reflect more than one frequency and sometimes a few pseudo components too. Several versions of EMD are proposed in the literature to alleviate this issue. One of the most popular techniques and among them is the EMD with intermittency criteria, originally proposed by Yang *et al.*<sup>19</sup> to capture the intermittent components in the signal. Later Gao *et al.*<sup>26</sup> proposed an alternative approach and eventually, several investigations are performed by the researchers to improve the EMD for extracting IMFs. Since the basic requirement of the proposed modal identification technique is to extract the true IMFs so that they represent the individual modal response, an EMD process with intermittency criteria is implemented. The details of the present decomposition process are detailed below.

An intermittent frequency  $f_i$  is imposed in the sifting process in such a way, that every IMF generated consists of only one frequency component in it. A band-pass filter is used during the sifting process to retain only the desired single frequency component,  $f_i$  in the IMF and eliminate the rest of the frequency components. Initially, the frequency spectrum details of the signal are obtained by performing the Fast Fourier Transform (FFT). The identified resonant frequencies of the structure from the frequency spectrum are divided into  $n_m$  number of partitions such that each partition contains only one resonant frequency  $f_k^0$ . Accordingly the starting and ending points of each partition (i.e.,  $f_k^u$  and  $f_k^l$  ( $k = 1, 2, 3, \dots, n_m$ )) are fixed as  $(1 \pm 5\%) f_k^0$ .  $\Omega_j = \{f \mid f_i \leq f \leq f_{j+1}\} \quad j = 1, 2, \dots, n_m \quad \dots (26)$

The band-pass filter is employed to generate a narrowband signal from each of the IMFs derived

from the original signal. The frequency components contained in these narrowband signals generated using the above-outlined procedure correlated strongly with the original signal. Hence true IMFs can be identified based on correlation strength. To retain the low amplitude true IMFs, both the signal as well as the narrowband signals are normalized before evaluating the correlation coefficients of the narrowband signals. The threshold  $\mathcal{G}$  defined as,  $\mathcal{G} = \max(v_i) / \kappa$  ( $i=1, \dots, n_{IMF}$ ), where  $\kappa > 1.0$  is an empirical factor. In the present work  $\kappa$  is taken as 10.0.

While all the pseudo-IMFs identified using the criteria  $v_i < \mathcal{G}$  are added to the residue, the rest of the IMFs are retained. Therefore, the proposed intermittency based modal decomposition technique meets the prime requirement of extracting all IMFs of the resonant modes and eliminating the rest of the pseudo decomposed signals. To alleviate the problem associated with the end effects during the sifting process of EMD, a time series based signal extension method is proposed. A wide variety of methods proposed in the literature to address this problem can be broadly classified as signal extension and extrema extension techniques.<sup>27</sup> However, these techniques will not work for non-stationary signals and are suitable only for periodic or quasi-periodic signals. Because of this, an AR model-based signal extension technique is employed in this paper, which can effectively cater to non-stationary and transient signals. The details are as follows:

Let  $Y = [y(t_1), y(t_2), \dots, y(t_n)]$ , a time series of size  $n$  and  $Y_{ext} = [y(t_{n+1}), \dots, y(t_{n+n_e})]$ , the extrapolated signal of size  $n_e$  can be computed as follows:

Set  $Y_s = Y - \mu$  to shift the mean of the signal,  $Y$ , to zero, where  $\mu$  is an average of the last  $p$  points *i.e.*,  $mean[y(t_{n-p}), y(t_{n-p+1}), \dots, y(t_n)]$ . Then extended points  $Y_{ext}$  are extrapolated by recursively using the two preceding points as

$$y_s(t_i) = \alpha_1 \cdot y_s(t_{i-1}) + \alpha_2 \cdot y_s(t_{i-2}) \quad \dots (27)$$

$$\forall i \in \{(n+1), \dots, n+n_e\},$$

$$Y_{ext} = (y(t_{n+1}), y(t_{n+2}), \dots, y(t_{n+n_e})) \quad \dots (28)$$

$$= (y_s(t_{n+1}), y_s(t_{n+2}), \dots, y_s(t_{n+n_e})) + \bar{y}$$

where,  $\alpha_1 = \frac{2 - (\omega_s \Delta t)^2}{(1 + \zeta \Delta t / 2)}$ ,  $\alpha_2 = \frac{(1 - \zeta \Delta t / 2)}{(1 + \zeta \Delta t / 2)}$  ... (29)

$\omega_s$  is the pulsation of the sinusoidal extension and it is determined as,

$$\omega_s = \begin{cases} \frac{\pi}{|T|} & \text{if } T \geq 4\Delta t \\ \frac{\pi}{4\Delta t} & \text{otherwise} \end{cases} \quad \dots (30)$$

where,  $T$  is the difference between the two-time instants of the last two extrema in the time series,  $\Delta t$  is the time step length *i.e.*  $t_2 - t_1$ .  $\zeta$  is the damping coefficient. It should be mentioned here that  $\omega_s$  is calculated based on the suggestion of Coughlin *et al.*<sup>28</sup> To avoid the autoregressive time series model from diverging to infinity, the value of  $T$  should always be greater than  $4\Delta t$ . Hence in Eq. (31), we need to set  $T$  as  $4\Delta t$ , if the value of  $T$  is less than  $4\Delta t$  the autoregressive model will automatically adjust the phase and amplitude of the sinusoidal extension. This model is capable of flattening the envelopes in the IMFs generated for low frequencies.

**Construction of Mode Shapes**

The mode shape of the structure associated with each identified frequency can be constructed by employing EMD and Hilbert transform on the measured vibration responses at several appropriately chosen spatial locations. The measured time history response  $z_m(t)$  can be decomposed into IMFs using the earlier outlined EMD procedure (*i.e.*, each IMF corresponds to a response of each structural mode),  $z^j_p(t)$  for  $j = 1, 2, 3, \dots, n$ . We use Hilbert transform on each modal response  $z^j_p(t)$  to evaluate the instantaneous parameters like phase  $\Phi^j_p(t)$  and amplitude,  $A^j_p(t)$ . Once these instantaneous values of each modal response are obtained, we can generate mode shapes using the following procedure.

The absolute values  $\Phi^j_{rs}$  and  $\Phi^j_{qs}$  ( $r, q = 1, 2, \dots, n$ ) of the  $j^{\text{th}}$  mode can be written as

$$\left| \frac{\Phi^j_{rs}}{\Phi^j_{qs}} \right| = \exp \left[ \tilde{A}^j_{rs}(t_0) - \tilde{A}^j_{qs}(t_0) \right] \quad \dots (31)$$

Similarly, the phase angle difference between  $\Phi^j_{rs}$  and  $\Phi^j_{qs}$  ( $r, q = 1, 2, 3, \dots, n$ ) of the  $j^{\text{th}}$  mode is

$$\theta(\Phi^j_{rs}) - \theta(\Phi^j_{qs}) = \theta^j_{rs}(t_0) - \theta^j_{qs}(t_0) \quad \dots (32)$$

We can use the least square straight line of the time history plots of  $\ln A_{rs}^j(T)$  and  $\ln A_{qs}^j(T)$  to arrive at the values of  $\tilde{A}_{rs}^j(t_0)$  and  $\tilde{A}_{qs}^j(t_0)$  at time  $t=t_0$ . Similarly, we can make use of the magnitudes of the least square straight lines of the phase angle  $\theta_{rs}^j(t)$  and  $\theta_{qs}^j(t)$  at time  $t=t_0$  to arrive at the values of  $\theta_{rs}^j(t_0)$  and  $\theta_{qs}^j(t_0)$  respectively. We can take  $t_0$  as a mid-point in the range of time in which the data  $\theta_{rs}^j(T)$  and  $\theta_{qs}^j(T)$  are available. Using this procedure (Eqs (31) and (32)) the absolute values and phase angle of all the modal elements relative to an arbitrary element can be evaluated. Using these relationships given in Eqs (31) and (32), the modal coordinates for each associated frequency can be obtained.

**Results and Discussion**

The investigations carried out on the proposed algorithm are organised into two phases. The first phase is a numerical simulation carried out to evaluate the proposed EMD process with intermittency along with the technique to handle end effects during sifting. For this purpose, a six-storey framed structure with closely spaced modes is deliberately chosen. The frame is modelled as a shear building with stiffness of each storey as  $K_1 = 2.0 \times 10^7$  N/m;  $K_2 = 4.0 \times 10^7$  N/m;  $K_3 = 6.0 \times 10^7$  N/m;  $K_4 = 8.0 \times 10^7$  N/m;  $K_5 = 1.0 \times 10^8$  N/m;  $K_6 = 1.2 \times 10^8$  N/m. The mass of each storey is 2000 Kg with the additional mass of 48000 Kg in the 3<sup>rd</sup> and 5<sup>th</sup> storey respectively. The natural frequencies of the system are 2.329 Hz; 5.840 Hz; 16.252 Hz; 35.408 Hz and 36.105 Hz. It can be observed that the fourth and fifth frequencies are very close and similarly the first two frequencies are reasonably close.

The sampling frequency is considered as 2000 Hz. The time history response of the acceleration at the top floor for 2000 time steps and the corresponding FFT spectra are shown in Fig. 1. As discussed earlier, we have used the AR model for handling the end effects in empirical mode decomposition. The extended signal using the formulations presented in the earlier sections to minimize the end effects associated with empirical mode decomposition. the extended portion of the signal is also shown in Fig. 1(a). The intrinsic mode functions (IMF) using the conventional and the proposed EMD procedures are shown in Fig. 2 along with their corresponding FFT spectra for the first two IMFS belonging to the closely

spaced frequencies. Even though more IMFs are generated using EMD, we have presented only the first two IMFs for comparison purposes. It can be easily verified from the FFT spectra of each IMF given in Fig. 2(a), that mode mixing is clearly present. Alternatively, the EMD with the proposed intermittency criteria is presented in Fig. 2(b) along with the corresponding FFT spectra. It can be verified from the FFT plots given in Fig. 2(b) that they are comparing very well with the corresponding frequency component of the original signal given in Fig. 1(b). It can be concluded from these investigations that the proposed EMD with intermittency criteria is effective in generating IMFs without mode mixing and can separate the closely spaced modes. The second phase is considered to test and verify the accuracy as well as practical amenability of the proposed technique. For this purpose, a practical example of a GNTVT tower with the measured time history responses is presented.<sup>29</sup>

The Guangzhou New TV Tower (GNTVT), of China, is shown in Fig. 3.<sup>(29-31)</sup> The total height of the tower is 600 m. While the main tower is 454 m high, the height of the antenna mast mounted over the tower is 156 m. The main tower is a tube-in-tube structure. The outer structure has a hyperboloid plan form and is

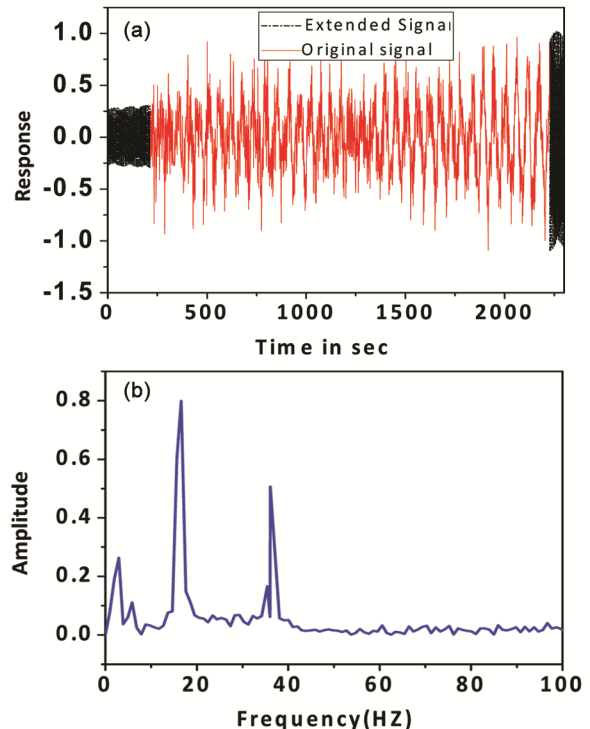


Fig. 1 — Time history response with extensions using AR and of six-storey framed structure and FFT spectra

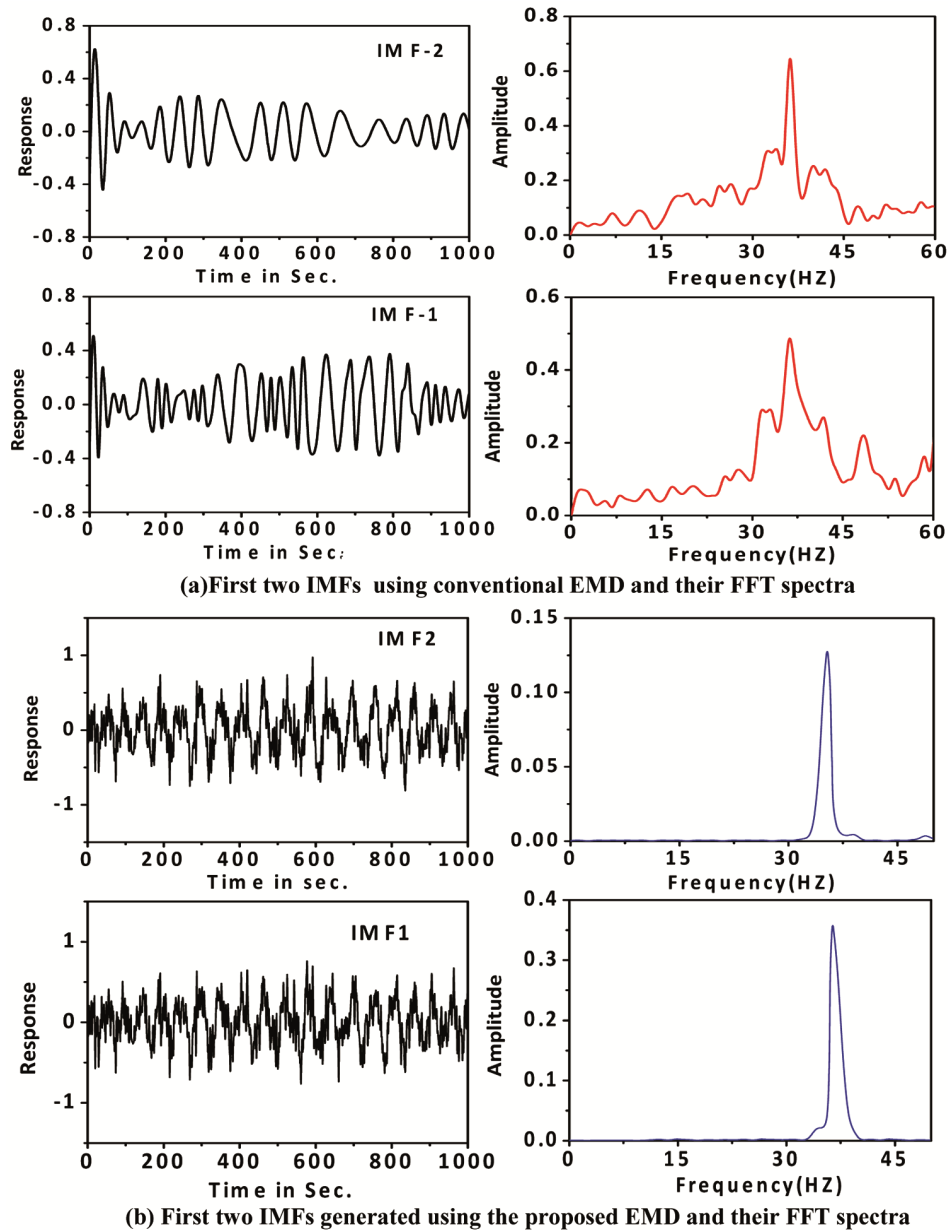


Fig. 2 — Performance of the proposed EMD with intermittency : (a) First two IMFs using conventional EMD and their FFT spectra; (b) First two IMFs generated using the proposed EMD and their FFT spectra

built with twenty-four steel tube columns with concrete fill, interconnected by transverse steel bracings and also steel beams. The ground level cross-sectional dimensions of the outer tower are  $50 \times 80$  m. While waist level dimensions are  $20.65 \times 27.5$  m, the top level has  $41 \times 55$  m. The inner structure is elliptical in shape, with cross-sectional dimensions of  $14 \times 17$  m. The inner structure is built with reinforced concrete with uniform cross-sectional dimensions all through the height. The 1800 Tons heavy steel antenna mast

(octagonal-shaped steel lattice structure) is mounted on the top of the tower.

The 3D finite element model of GNTVT, with 5 05 164 Degrees of freedom (DF) based on detailed available drawings is developed in ANSYS commercial finite element software and it is found to be too large. Because of this, a reduced-order model is developed and reported in the literature.<sup>29</sup> The reduced-order model is calibrated with the experimental results. The reduced FEM model is idealized as a cantilever with 37 beam elements and

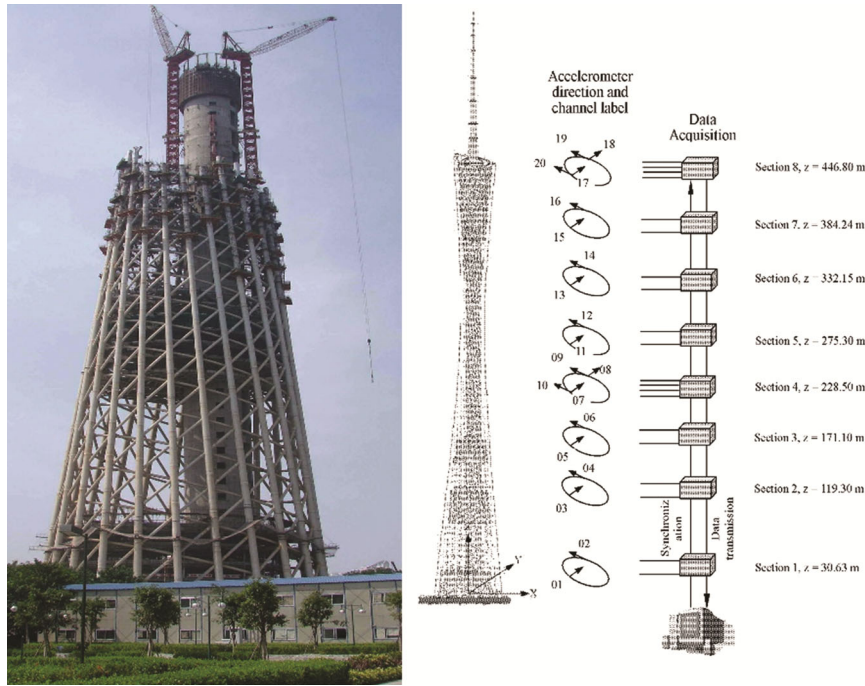


Fig. 3 — The GNTV tower in Guangzhou, China and its data acquisition system<sup>26</sup>

38 nodes.<sup>29</sup> Since the axial DF is constrained at each node, the active DF at each node works out to five (2 translational and 3 rotational). The complete details related to the reduced-order model, global system matrices of the reduced FEM model are given in the benchmark webpage.<sup>31</sup>

More than 700 sensors are reported to be installed in the GNTVT tower and is being considered currently as an SHM benchmark problem for high-rise slender structures.<sup>29,30</sup> To acquire acceleration time history data of the tower subjected to ambient wind excitations or earthquake excitations, twenty uni-axial accelerometers are installed on the tower. The acceleration time history data is reported to be collected at a sampling rate of 50 Hz. As shown in Fig. 3, accelerometers are installed at eight different levels. While two accelerometers are installed at each level to measure acceleration time history data in two orthogonal directions, four accelerometers are installed (i.e., two for the long axis and two for the short axis) at the fourth and eighth levels. The measured vibration data from the ambient wind excitations of the GNTVT are made publicly available<sup>31</sup> and is used in the present work for modal parameter estimation using the proposed HHT based algorithm. Detrending and resampling of the time history data are carried out as discussed in Lakshmi *et al.*<sup>10</sup> before carrying out the modal

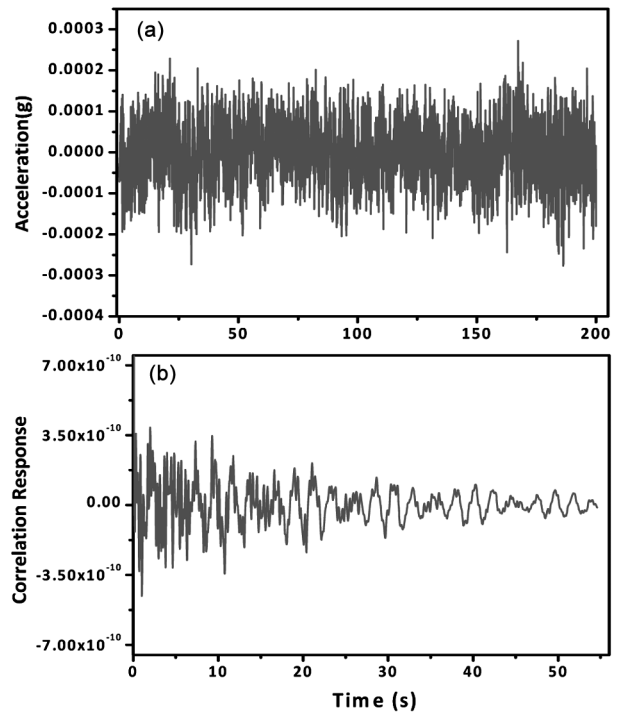


Fig. 4 — Typical time history and cross-correlated responses of GNTVT: (a) Acceleration time history; (b) Free response through cross-correlation

identification process using the proposed algorithm. A typical time history response and also correlated response is shown in Fig. 4.

EMD with intermittency criteria discussed in one of above section is employed to decompose the impulse responses to arrive at intrinsic mode functions (IMFs). Performing HT on each IMF, the instantaneous parameters like amplitude and phase as a function of time are evaluated. Plots related to ‘phase angle  $\theta_{rs}^j$  Vs time’ and ‘ $\ln A_{rs}^j(T)$  Vs time’ for a typical IMF (modal response) is shown in Fig. 5. As expected, the instantaneous phase and log of instantaneous amplitude oscillate around the straight lines. As discussed in section 2.2, the least-square fit of the two curves are generated and are shown as straight lines in Fig. 5. The slope of the least square fit line in the ‘phase angle  $\theta_{rs}^j$  Vs time’ plot given in Fig. 5 (a) is the damped natural frequency  $\omega_d^j$  associated with a typical  $j^{\text{th}}$  IMF. Similarly, the slope of the least square fit line of the ‘ $\ln A_{rs}^j(T)$  Vs time’ plot of a typical  $j^{\text{th}}$  IMF given in Fig. 5(b), is the decaying amplitude  $-\zeta_j \omega_n^j$ . The natural frequency and damping ratios can be obtained from Eqs (24) and (25), using the parameters  $\omega_d^j$  and  $-\zeta_j \omega_n^j$  evaluated for each

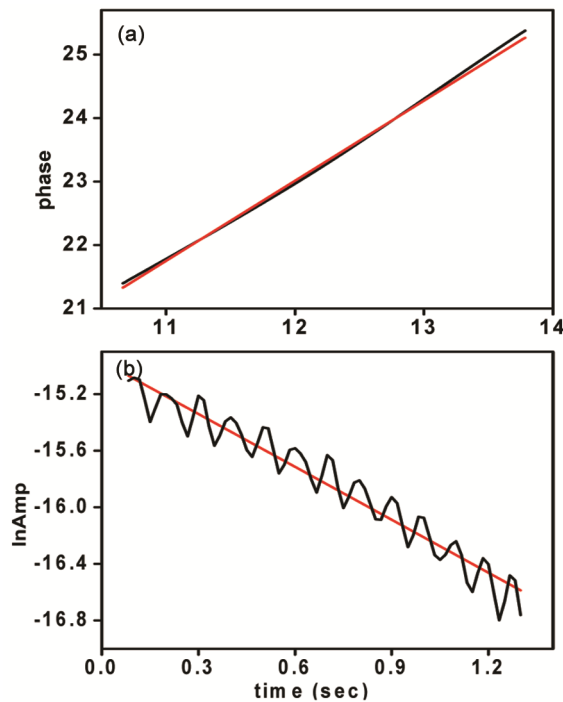


Fig. 5 — Instantaneous amplitude and phase plots of a typical IMF for modal parameter extraction of GNTVT tower: (a) Instantaneous Phase Vs Time plot; (b) log of Instantaneous amplitude Vs time plot Evaluated using HHT FEM

IMF (modal response) as detailed in section 2.1. The mode shapes associated with each frequency are constructed using the vibration data from all the spatially located sensors as described in above section. Since 90 data sets are considered for modal identification, average values of natural frequencies and damping ratios are shown along with the theoretical FEM results in Table 1. The mode shapes for the tower constructed using the proposed algorithm is shown in Fig. 6 along with theoretical (FEM) results. A close agreement can be observed between the estimated and the theoretical mode shapes.

Table 1 — Modal identification of GNTVT using HHT based algorithm

S. NO	FEM	Proposed HHT based algorithm	
	Frequency (Hz)	Frequency (Hz)	Damping Ratio
1	0.1104	0.0944	1.0263
2	0.1587	0.1395	0.9691
3	0.3463	0.3620	1.2082
4	0.3688	0.4192	0.3402
5	0.3994	0.4728	0.2305
6	0.4605	0.5044	0.3898
7	0.4850	0.5219	0.3529
8	0.7380	0.7862	0.3628
9	0.9026	0.9597	0.3208
10	0.9972	1.0435	0.3104

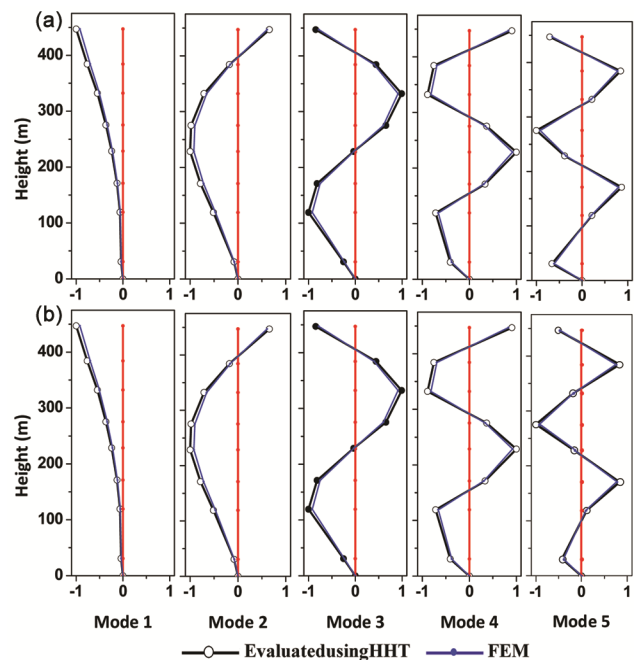


Fig. 6 — Evaluated modes of the GNTVT using the HHT based algorithm: (a) In X-Direction; (b) In Y-Direction

## Conclusions

An improved version of HHT based algorithm for modal identification of practical engineering structures is proposed in this paper. EMD with intermittency criteria, which handles mode mixing due to closely spaced modes, is used on the free responses obtained using cross-correlation of measured vibration responses. Each IMF obtained using EMD can be construed as the modal response of the corresponding mode. The frequencies and damping ratios are obtained by applying the Hilbert transform on each modal response. The mode shapes are obtained by similarly processing the data from all spatially located sensors. An efficient technique to handle the end effects during sifting is also suggested.

Investigations carried out using a numerical framed structure and the publicly available measured acceleration time history data of ambient wind excited GNTVT, indicate that the proposed HHT-based technique can handle closely spaced modes and is highly amenable to employ for large structures.

## Acknowledgement

This paper is being published with the permission of the Director, CSIR-SERC, Chennai.

## References

- Huang C S & Yeh C H, Some properties of Randomdec signature, *Mech Syst Signal Process*, **13(3)** (1999) 491–506.
- Ibrahim S R & Pappa R S, Large modal survey testing using the Ibrahim time domain identify technique, *J Spacecr Rockets*, **19(5)** (1982) 459–465.
- Vold H & Russell R, Advanced analysis methods improve modal test results, *J Sound Vib*, **17(3)** (1983) 36–40.
- Liu T Y & Chiang W L, Chen C W, Hsu W K, Lu L C & Chu T J, Identification and monitoring of bridge health from ambient vibration data, *J Vib Control*, **17(4)** (2011) 589–603.
- Lardies J, Modal parameter identification based on ARMAV and state-space approaches, *Arch Appl Mech*, **80(4)** (2010) 335–352.
- Ali M R & Okabayashi T, System identification of highway bridges from ambient vibration using subspace stochastic realization theories, *Earthq Struct*, **2(2)** (2011) 189–206.
- Caicedo J M, Practical guidelines for the natural excitation technique (NEXT) and the Eigen system realization algorithm (ERA) for modal identification using ambient vibration, *Exp Tech*, **35(4)** (2011) 52–58.
- Lakshmi K, Reddy V K, & Rao A R M, Modal Identification of practical engineering structures using second-order blind identification, *J Inst Eng (India): A*, **102(2)** (2021) 499–512.
- Ghrib F & Li L, An adaptive filtering-based solution for the Bayesian modal identification formulation, *J Civ Struct Health Monit*, **7(1)** (2017) 1–13.
- D, Lei Y, Yu E & Wallace J, Identification, model updating and response prediction of an instrumented 15-story steel-frame building, *Earthq Spectra*, **22(3)** (2006) 781–802.
- Ni P, Li J, Hao H, Xia Y, Wang X, Lee J M & Jung K H, Time-varying system identification using variational mode decomposition, *Struct Control Health Monit*, **25(6)** (2018) e2175.
- Yang Y, Peng Z, Zhang W & Meng G, Parameterised time-frequency analysis methods and their engineering applications: a review of recent advances, *Mech Syst Signal Process*, **119** (2019) 182–221.
- Mahato S, Teja M V & Chakraborty A, Combined wavelet–Hilbert transform-based modal identification of road bridge using vehicular excitation, *J Civ Struct Health Monit*, **7(1)** (2017) 29–44.
- Huang N E, Shen Z, Long S R, Wu M C, Shih H H, Zheng Q, Yen N, Tung C C & Liu H H, The empirical mode decomposition and Hilbert spectrum for nonlinear and nonstationary time series analysis, *Proc R Soc A: Math Phys Eng Sci*, **454** (1971) (1998) 903–995.
- Yang J N & Lei Y, Identification of natural frequencies and damping ratios of linear structures via Hilbert transform and empirical mode decomposition, *Proc IASTED Int Conf Intell Syst Control* (IASTED/Acta Press, Anaheim, California) 1999, 310–315.
- Feldman M, Nonlinear free-vibration identification via the Hilbert transform, *J Sound Vib*, **208(3)** (1997) 475–489.
- Yang J N, Lei Y, Pan S & Huang N, System identification of linear structures based on Hilbert-Huang spectral analysis, Part 1: Normal modes, *Earthq Eng Struct Dyn*, **32(9)** (2003) 1443–1467.
- Yang J N, Lei Y, Pan S & Huang N, System identification of linear structures based on Hilbert-Huang spectral analysis Part 2: Complex modes, *Earthq Eng Struct Dyn*, **32(10)** (2003) 1533–1554.
- Yang J N, Lei Y & Huang N, Identification of natural frequencies and damping of in situ tall buildings using ambient wind vibration data, *J Eng Mech*, **130(5)** (2004) 570–577.
- Mao J X, Wang H, Feng D M, Tao T Y & Zheng W Z, Investigation of dynamic properties of long-span cable-stayed bridges based on one-year monitoring data under normal operating condition, *Struct Control Health Monit*, **25(5)** (2018) 1–19.
- Bagheri A, Ozbulut O E & Harris D K, Structural system identification based on variational mode decomposition, *J Sound Vib*, **417** (2018) 182–197.
- Huang N E, Huang K & Chiang W L, HHT-based bridge structural health-monitoring method, *Hilbert-Huang Transform and its Applications*, (2005) 263–285.
- Roveri N & Carcaterra A, Damage detection in structures under traveling loads by Hilbert–Huang transform, *Mech Syst Signal Process*, **28** (2012) 128–144.
- Elbouchikhi E V, Choqueuse Y, Amirat M, Benbouzid & Turri S, An efficient Hilbert-Huang Transform-based bearing faults detection in induction machines, *IEEE Trans Energy Convers*, **32(2)** (2017) 401–413.

- 25 Rao A R M & Lakshmi K, Damage diagnostic technique combining POD with time-frequency analysis and dynamic quantum PSO, *Meccanica*, **50(6)** (2015) 1551–1578.
- 26 Gao Y, Ge G, Sheng Z & Sang E, Analysis and solution to the mode mixing phenomenon in EMD, in *2008 Congr Image Signal Process*, **5** (2008) 223–227.
- 27 Shen S S P, Shu T, Huang N E, Zhaohua W U, North G R, Karl T R & Easterling D R, HHT Analysis of the nonlinear and non-stationary annual cycle of daily surface air temperature data, in cited by N E Huang & Samuel S P Shen *Hilbert-Huang Transform and its Applications*, (2005) 187–209.
- 28 Coughlin K, Tung K K, Empirical mode decomposition and climate variability, in *Hilbert-Huang Transform and its Applications*, cited by N E Huang & Samuel S P Shen, (2014) 223–239.
- 29 Chen W H, Lu Z R, Lin W, Chen S H, Ni Y Q, Xia Y, Liao W Y, Theoretical and experimental modal analysis of the Guangzhou New TV Tower, *Eng Struct*, **33(12)** (2011) 3628–3646.
- 30 Ni Y Q, Xia Y, Liao W Y & Ko J M, Technology innovation in developing the structural health monitoring system for Guangzhou new TV tower, *Struct Control Health Monit*, **16(1)** (2009) 73–98.
- 31 Xia Y, Ni Y Q, Ko J M & Chen H B, Development of a structural health monitoring benchmark problem for high-rise slender structures, *Adv Sci Technol*, **56** (2008) 489–494.